Supplementary Information (SI) for EES Solar.

Supplementary Information

Evaporated organic-MoO_3 composite hole transport layers toward stable perovskite solar cells

Jisu Hong,[a] Zhaojian Xu,[a] Tuo Hu,[a] Sujin Lee,[a] Manting Gui,[a] Antoine Kahn,[a] Barry P. Rand[ab]*

[a] Department of Electrical and Computer Engineering, Princeton University, Princeton, New Jersey 08544, United States

[b] Andlinger Center for Energy and the Environment, Princeton University, Princeton, New Jersey 08544, United States

* Email: brand@princeton.edu (B. P. Rand)

Experimental Methods

Materials

2,2',7,7'-tetra(N,N-di-p-tolyl)amino-9,9-spirobifluorene (spiro-TTB, > 99%), 2,2',7,7'-tetrakis[N,N-di(4-methoxyphenyl)amino]-9,9'-spirobifluorene (spiro-OMeTAD, > 99.5%), 4,4',4''-tris[(3-methylphenyl)phenylamino]triphenylamine (m-MTDATA, > 99.5%), and tris(2-(1H-pyrazol-1-yl)-4-tert-butylpyridine)-cobalt(III)tris(bis(trifluoromethylsulfonyl)imide)) (FK209 Co(III) TFSI, > 99%) were purchased from Lumtec. Molybdenum(VI) oxide (MoO_3, 99.95%) and tin(IV) oxide (SnO_2, 15% in H_2O colloidal dispersion) were purchased from Alfa Aesar. Lead iodide (PbI_2, 99.99% trace metal basis) was purchased from TCI. Formamidinium iodide (FAI, > 99.99%), methylammonium chloride (MACl, > 99.99%), and 4-methoxy-phenethylammonium iodide (MeO-PEAI) were purchased from GreatCell Solar. Methylenediamine dihydrochloride ($MDACl_2$, ≥ 98%), potassium chloride (KCl, 99.0%–100.5%), and lithium bis(trifluoromethane)sulfonimide (LiTFSI, 99.95%) were purchased from Sigma-Aldrich. Au (99.99%) and Ag (99.99%) were purchased from Kurt J. Lesker. N,N-dimethylformamide (DMF, anhydrous, 99.8%), dimethyl sulfoxide (DMSO, anhydrous, ≥ 99.9%), ethyl ether (anhydrous), chlorobenzene (CB, anhydrous, 99.8%), 2-propanol (IPA, anhydrous, 99.5%), acetonitrile (ACN, anhydrous, 99.8%), and 4-tert-butylpyridine (*t*-BP, 98%) were purchased from Sigma-Aldrich. All materials and solvents were used as received without further purification.

Fabrication and characterization of composite hole transport layers

Composite films of Spiro-TTB:MoO_3 were fabricated by co-evaporation of spiro-TTB and MoO_3, where the volume ratios were controlled by deposition rates of two sources and the total deposition rate was 1 $Å\ s^{-1}$. The pristine spiro-TTB and spiro-TTB:MoO_3 composite films with a thickness of 100 nm were deposited on Si substrates for morphology characterization. Atomic force microscope (AFM) images of spiro-TTB:MoO_3 composite films were obtained using a VEECO Dimension 3100 Atomic Force Microscope operated at tapping mode. For the ultraviolet photoelectron spectroscopy (UPS) study, performed to determine the energy level of composite films, 10 nm of the spiro-TTB and the spiro-TTB:MoO_3 films were deposited on indium tin oxide (ITO)-coated glass substrates. UPS measurements were performed under ultrahigh vacuum conditions (10^{-10} Torr) at room temperature, using He I photons (21.22 eV) produced by a discharged lamp. A bias of -5 V was applied to measure the secondary electron cutoff. The experimental energy resolution for the UPS measurements was 0.10 eV. The Fermi level reference in UPS measurement was calibrated using the Fermi edge of a clean Au substrate. For the conductivity measurement, 100 nm of the spiro-TTB and the composite films were deposited on bare glass substrates, followed by Au electrode deposition. The Au interdigitated electrodes have 15 gaps, a channel length of 150 μm, and a channel width of 5 mm. Current density-voltage (*J-V*) curves were measured using probe tips connected to a Keithley 2400 instrument in an ambient atmosphere to measure the conductivity, while conductivity-time graphs were recorded in an iodine-rich atmosphere to evaluate the stability towards iodine doping.

Fabrication and measurement of perovskite solar cells

ITO-coated glass substrates were cleaned by sonication in deionized water, acetone, and 2-propanol, and the residual solvents were blow-dried using pressured nitrogen. The oxygen plasma treatment was performed before the spin-coating of the SnO_2 layer. The SnO_2 solution was prepared by diluting the SnO_2 particle dispersion with a concentration of 15 wt% with deionized water to 2.67 wt%. The diluted SnO_2 solution was spin-coated on the substrates at 4000 rpm for 30 s with acceleration of 1000 rpm, followed by annealing at 150 °C for 30 min. The KCl solution at 5 mg mL^{-1} in deionized water was prepared and spin-coated at 5000 rpm with acceleration of 2000 rpm for 30 s. The KCl layer was annealed at 150 °C for 15 min, and treated by O_2 plasma for 10 min before the formamidinium lead iodide ($FAPbI_3$) layer deposition. The $FAPbI_3$ solution was prepared by dissolving perovskite precursors and additives, which were 583 mg of PbI_2, 217 mg of FAI, 30 mg of MACl, and 6 mg of $MDACl_2$, in 800 μL of DMF and 100 μL of DMSO. The solution was stirred and heated at 60 °C for more than 10 min and filtered with a 45 μm-polytetrafluoroethylene (PTFE) filter before spin-coating. The $FAPbI_3$ layer was deposited by a three-step spin-coating recipe including spin coating at 400 rpm for 4 s, 900 rpm for 6 s, and 2000 rpm for 20 s. 1 mL of diethyl ether as an antisolvent was dropped on the substrates 8 s before the final step ended. The perovskite layer was then annealed at 120 °C for 50 min. The MeO-PEAI surface treatment layer was deposited by preparing MeO-PEAI in IPA solution (4.5 mg mL^{-1}), filtering the solution with a 45 μm-PTFE filter, and spin-coating at 5000 rpm (2000 rpm acceleration) for 30 s, followed by annealing at 100 °C for 5 min. Three different recipes were used for the different hole transport layers (HTLs); control, double, and composite HTLs. For the control HTL, spiro-OMeTAD solution was prepared by dissolving 94 mg of spiro-OMeTAD in 1.1 mL of chlorobenzene, mixed with 37 μL of t-BP, 23 μL of LiTFSI solution (516.75 mg mL^{-1} in ACN), and 9 μL of CoTFSI solution (375.75 mg mL^{-1} in ACN). This solution was filtered with a 45 μm-PTFE filter and spin-coated at 3500 rpm with 1000 rpm acceleration for 30 s. For the double HTL, the concentration of the spiro-OMeTAD solution was diluted to 30 mg mL^{-1} for the thin spiro-OMeTAD layer, and spin-coated at the same spin speed. After that, the 100 nm of spiro-TTB:MoO_3 layer was deposited by co-evaporation of the spiro-TTB and MoO_3 at deposition rates of 0.85 and 0.15 Å s^{-1}, respectively, in a vacuum chamber at pressure under 2×10^{-6} Torr. The composite HTL was fabricated by evaporating 5 nm of the spiro-TTB and co-evaporating 145 nm of the spiro-TTB:MoO_3 layer. Finally, a top electrode was deposited by thermal evaporation at 1 Å s^{-1}. The *J-V* curves of perovskite solar cells (PSCs) were measured using a solar simulator (ABET Technologies) calibrated for AM 1.5 G illumination, and a Keithley 2602B SourceMeter in an N_2-filled glovebox. The thermal stability test and 1-sun light illumination test were also conducted in an N_2-filled glove box without device encapsulation. EQE measurements were conducted using a Newport TLS-300X tunable light source. Monochromated light from a 250 W quartz tungsten halogen lamp was modulated by an optical chopper operating at 150 Hz. Modulated light went through long pass filters before illuminating on the device under test (DUT). DUT was always kept in a vacuum-sealed box, and was short-circuited throughout the measurement process. Photocurrent responses were acquired using a combination of a preamplifier and a lock-in-amplifier system (SR570 and SR830, Stanford Research Systems). The incident photon flux was quantified by a silicon photodetector (Newport) for calibration. The perovskite/HTL samples used for UV-vis absorption and photoluminescence (PL) measurements were fabricated on bare glass substrates, following the same perovskite and HTL fabrication protocols outlined for solar cell fabrication. UV-vis absorption spectra were measured by using an Agilent Cary 5000 UV-Vis-NIR Spectrophotometer. PL measurements were conducted using a fiber-coupled spectrograph (Princeton Instruments, SpectraPro HRS-300) equipped with a cooled silicon charge-coupled device detector (PIXIS 400B). The samples were excited by a 405 nm laser diode with a power density of 67 mW cm^{-2} (Thorlabs, DL5146-101S). The X-ray photoelectron spectroscopy (XPS) study was conducted on the Au top electrode peeled off from the PSCs using carbon tapes. The XPS spectra were measured by a Thermo-Scientific K-Alpha X-ray Photoemission Spectrometer operating at a base pressure of 5×10^{-8} mbar. Scanning electron microscope (SEM) images were measured by using Verios 460 Extreme High Resolution Scanning Electron Microscope operated at 10 kV. The samples were coated with iridium for the SEM measurement.

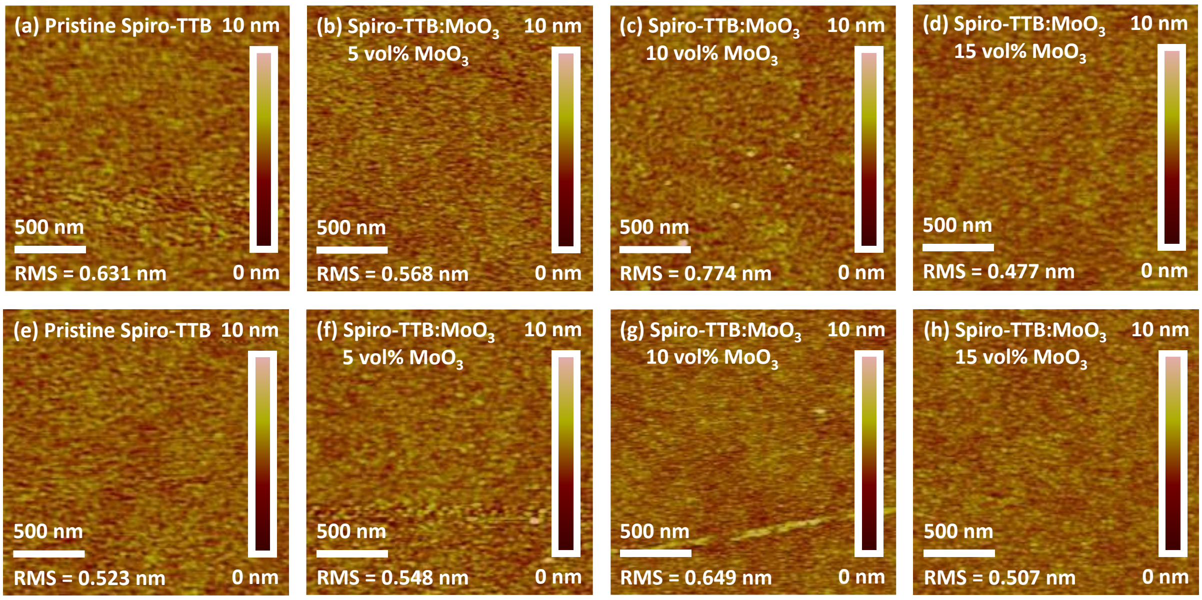

Fig. S1 AFM images of (a and e) the pristine spiro-TTB films and (b-d and f-h) the spiro-TTB:MoO$_3$ composite films (a-d) before and (e-h) after annealing at 70 °C for 1 h.

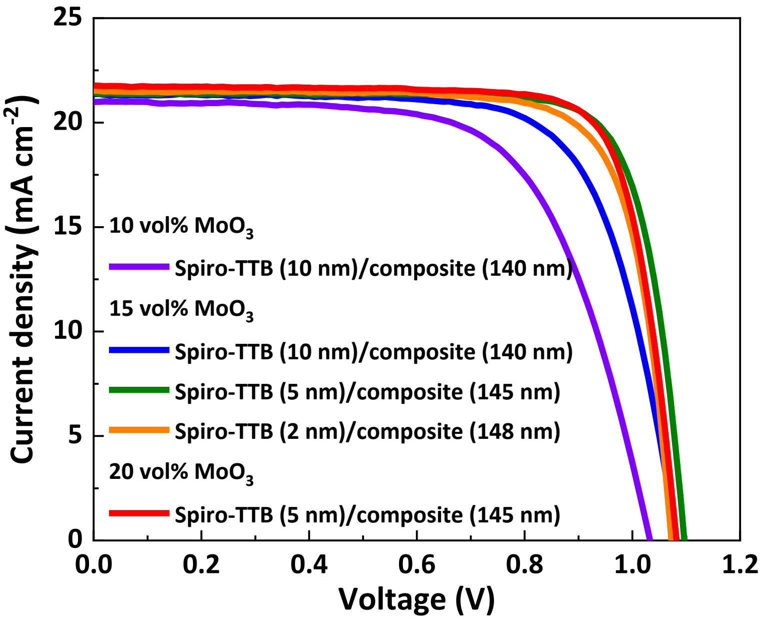

Fig. S2 *J-V* characteristics of the PSCs utilizing the spiro-TTB:MoO$_3$ composite HTLs with varying thicknesses and MoO$_3$ concentrations.

Table S1 Photovoltaic parameters of the PSCs incorporating the composite HTLs with different thicknesses and MoO_3 concentrations

HTL	V_{oc} (V)	J_{sc} (mA cm^{-2})	FF (%)	PCE (%)
Spiro-TTB (10 nm)/ composite (10 vol%, 140 nm)	1.02 (± 0.02)	21.0 (± 0.46)	63.5 (± 1.99)	13.6 (± 0.63)
Spiro-TTB (10 nm)/ composite (15 vol%, 140 nm)	1.08 (± 0.01)	20.7 (± 0.62)	71.9 (± 1.01)	16.1 (± 0.33)
Spiro-TTB (5 nm)/ composite (15 vol%, 145 nm)	1.10 (± 0.01)	20.9 (± 0.52)	79.7 (± 0.36)	18.3 (± 0.29)
Spiro-TTB (2 nm)/ composite (15 vol%, 148 nm)	1.08 (± 0.01)	21.0 (± 0.37)	77.6 (± 0.86)	17.6 (± 0.18)
Spiro-TTB (5nm)/ composite (20 vol%, 145 nm)	1.07 (± 0.02)	21.0 (± 0.82)	78.9 (± 1.09)	17.7 (± 0.69)

Table S2 Photovoltaic parameters of the PSCs with different HTLs measured in reverse scan

HTL	V_{oc} (V)	J_{sc} (mA cm^{-2})	FF (%)	PCE (%)
Control	1.13 (± 0.01)	21.9 (± 0.4)	80.8 (± 1.6)	20.0 (± 0.5)
Double	1.13 (± 0.02)	21.8 (± 0.4)	84.3 (± 1.5)	20.8 (± 0.4)
Composite	1.10 (± 0.01)	20.9 (± 0.5)	79.7 (± 0.4)	18.3 (± 0.3)

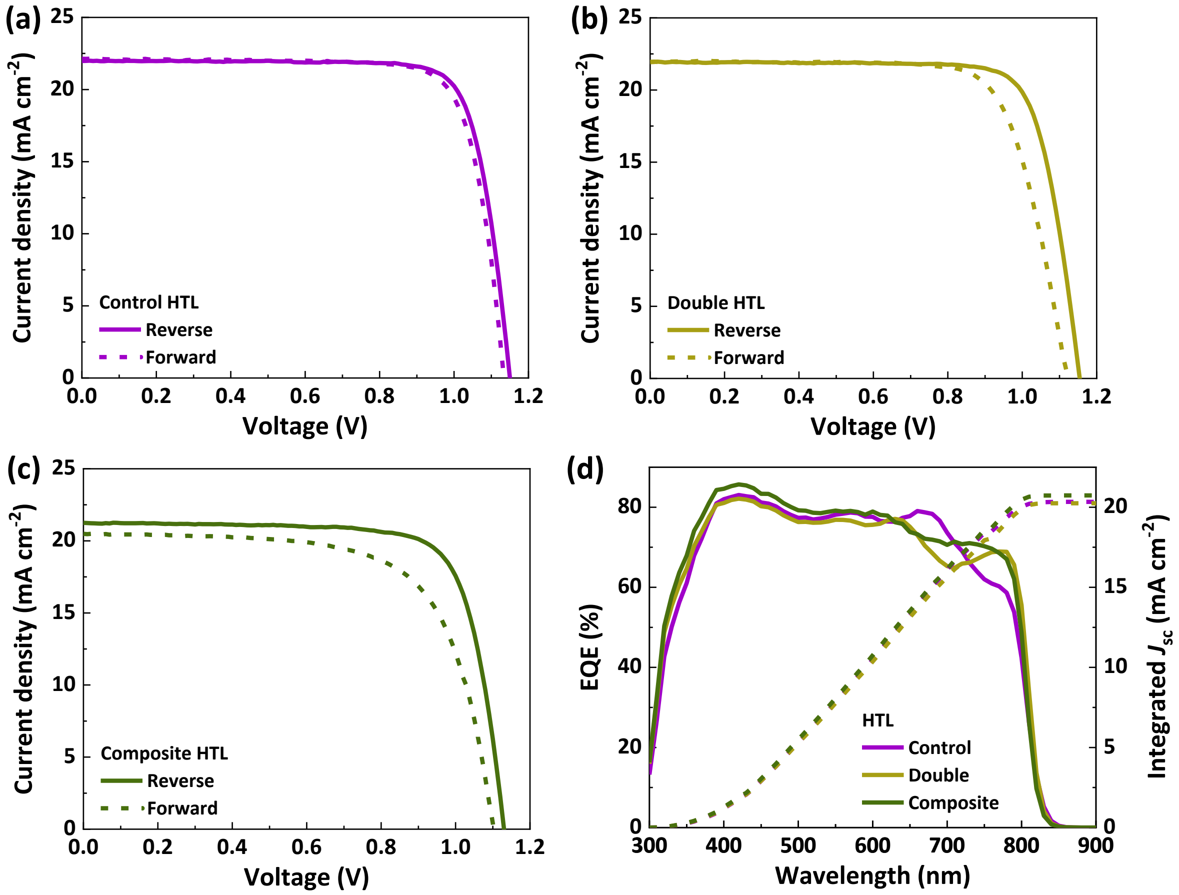

Fig. S3 (a–c) *J-V* characteristics of the PSCs with different HTLs measured in forward and reverse scan directions, and (d) EQE spectra and integrated J_{sc} values of the PSCs as a function of wavelength.

Table S3 Photovoltaic parameters of the PSCs measured in reverse and forward scans

HTL	Scan direction	V_{oc} (V)	J_{sc} (mA cm^{-2})	FF (%)	PCE (%)	Integrated J_{sc} (mA cm^{-2})
Control	Reverse	1.15	22.0	80.6	20.3	20.3
	Forward	1.13	22.1	79.4	19.8	
Double	Reverse	1.15	21.9	79.7	20.1	20.3
	Forward	1.12	22.0	74.8	18.4	
Composite	Reverse	1.13	21.3	76.5	18.4	20.7
	Forward	1.10	20.5	67.9	15.3	

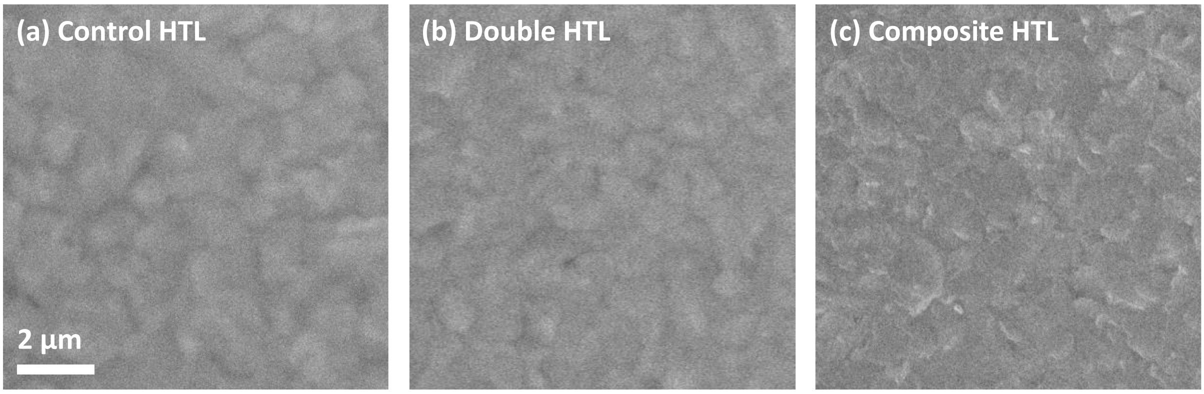

Fig. S4 Top-view SEM images of the HTLs deposited on the $FAPbI_3$ perovskite layers.

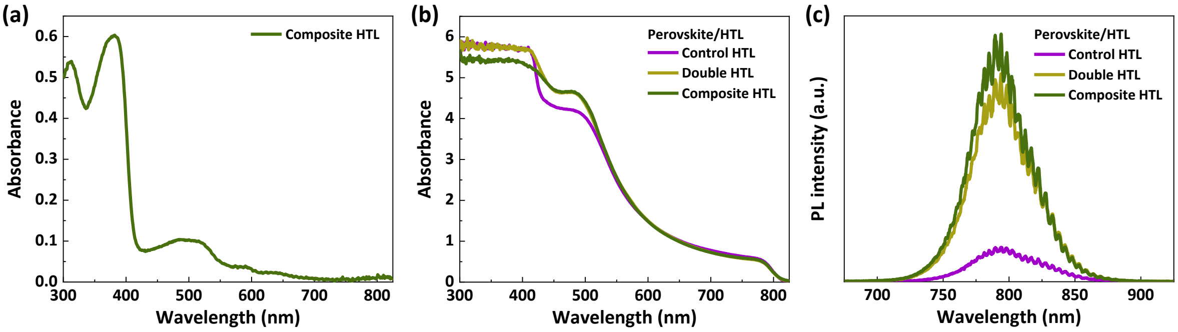

Fig. S5 (a-b) UV–vis absorption spectra of (a) the composite HTL film and (b) perovskite/HTL films on glass, and (c) photoluminescence spectra of perovskite/HTL films.

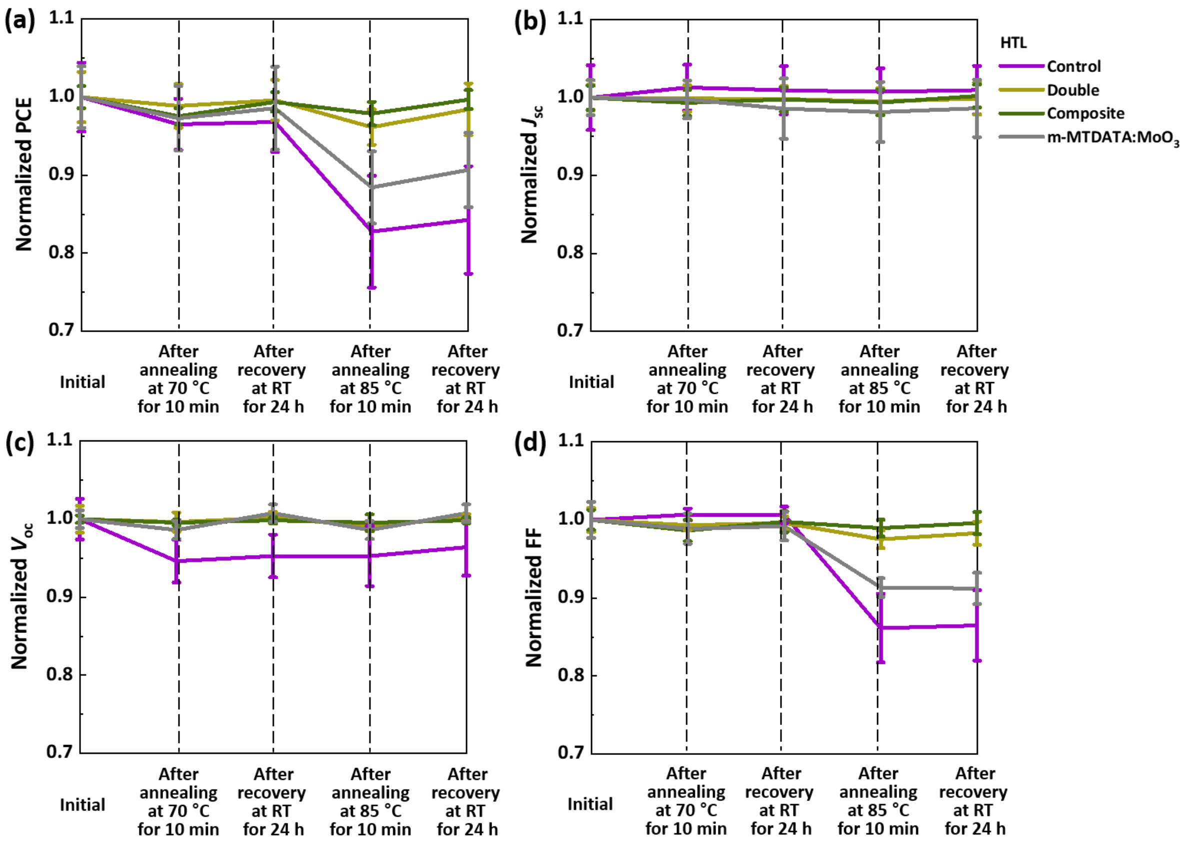

Fig. S6 Normalized (a) PCE, (b) J_{sc}, (c) V_{oc}, and (d) FF graphs of PSCs with different HTLs during the thermal stress test.

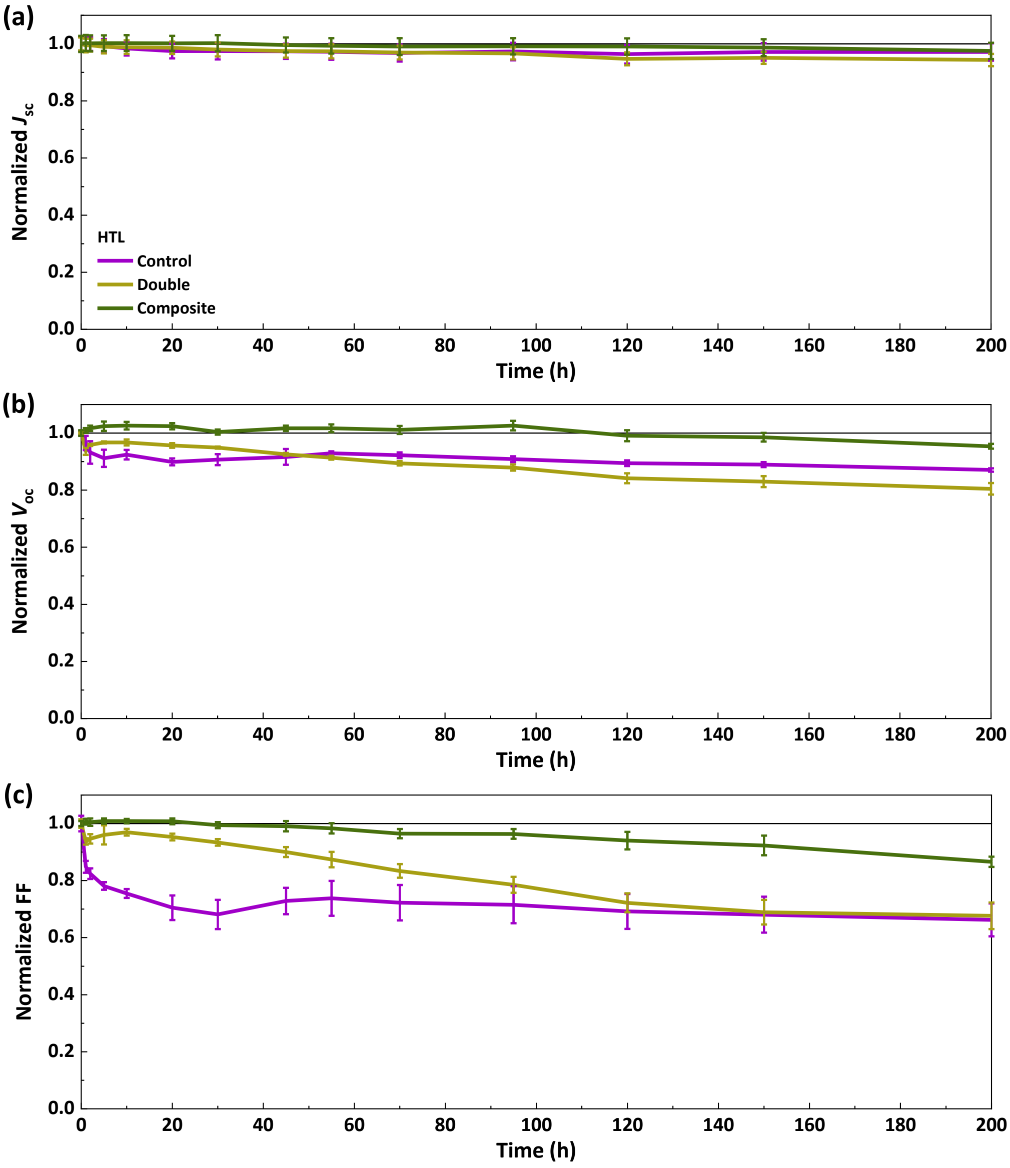

Fig. S7 Normalized (a) J_{sc}, (b) V_{oc}, and (c) FF graphs of PSCs fabricated in a dry condition (RH < 20%) and measured during the thermal stress test performed at 85 °C.

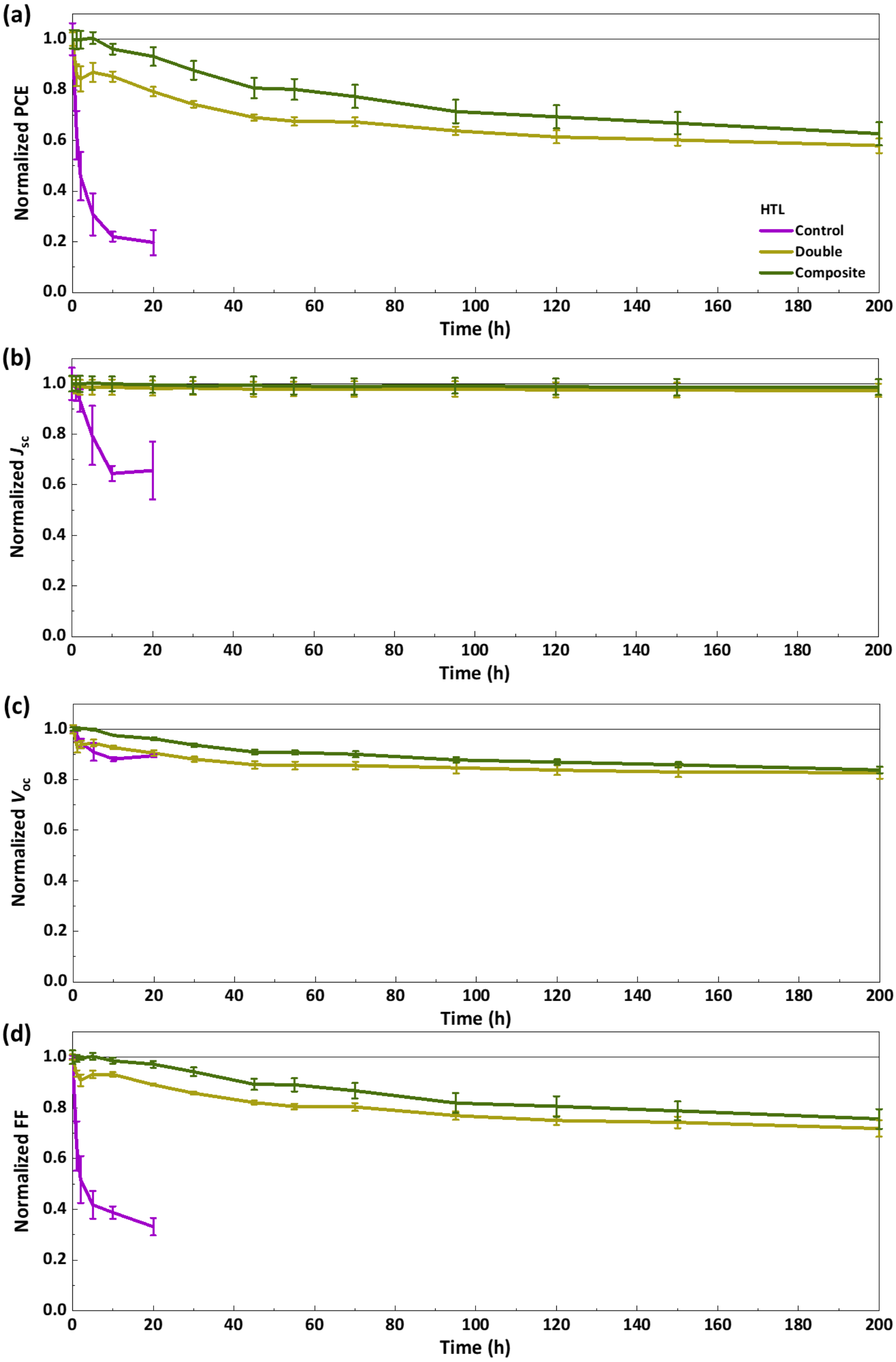

Fig. S8 Normalized (a) PCE, (b) J_{sc}, (c) V_{oc}, and (d) FF graphs of PSCs fabricated in a humid condition (40 % < RH < 45%) and measured during the thermal stress test at 85 °C.

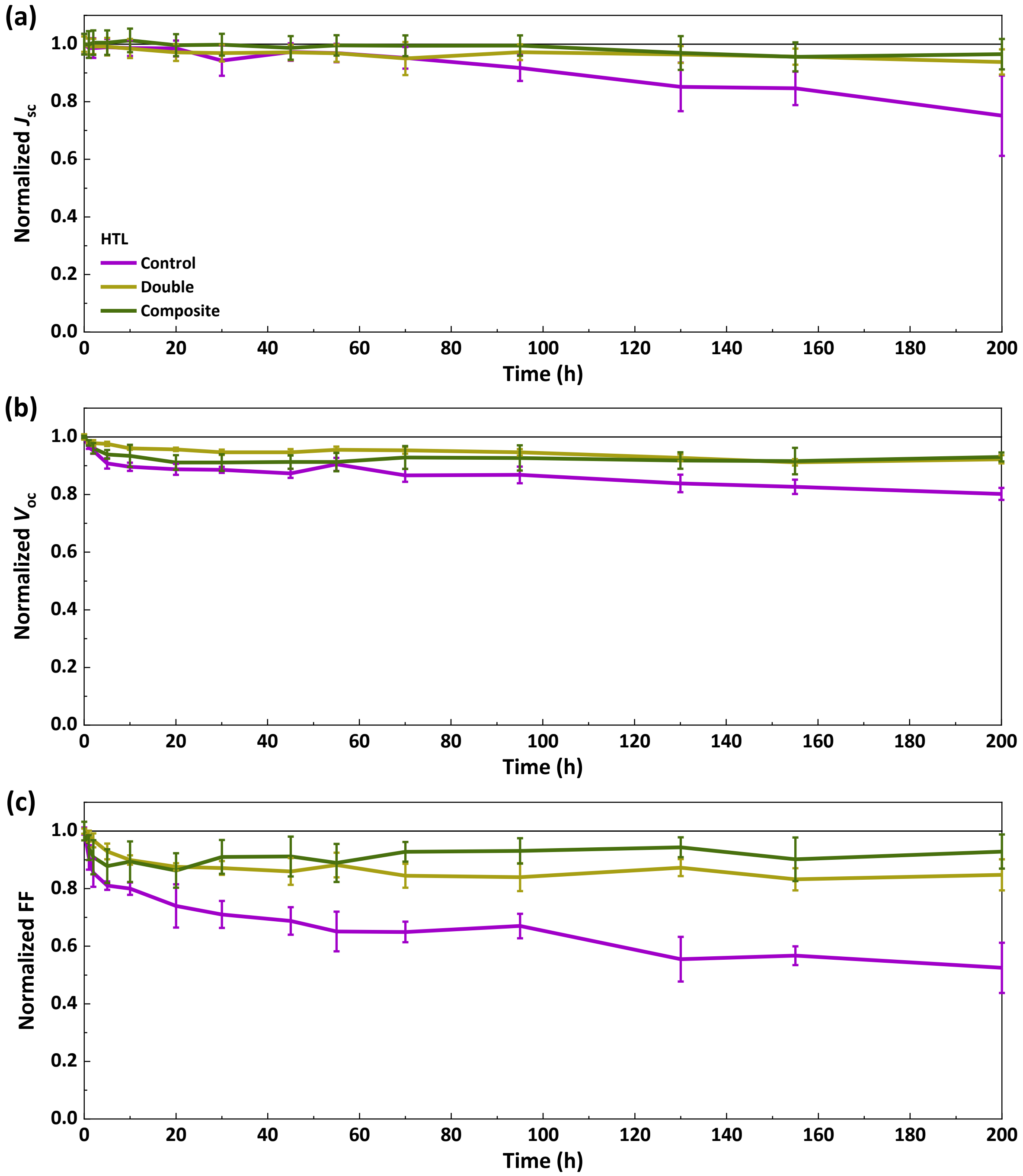

Fig. S9 Normalized (a) J_{sc}, (b) V_{oc}, and (c) FF of the PSCs measured during continuous 1-sun light illumination.